Electronic Supplementary Information (ESI)

Probing juxtaposed G-quadruplex and hairpin motifs using a responsive nucleoside probe: a unique scaffold for chemotherapy

Saddam Y. Khatik,[a] Sruthi Sudhakar,[b] Satyajit Mishra,[c] Jeet Kalia,[c,d] P.I. Pradeepkumar[b] and Seergazhi G. Srivatsan*[a]

[a]Department of Chemistry, Indian Institute of Science Education and Research (IISER), Pune. Dr. Homi Bhabha Road, Pune 411008, India; E-mail: srivatsan@iiserpune.ac.in.

[b]Department of Chemistry, Indian Institute of Technology Bombay, Mumbai 400076, India.

[c]Department of Biological Sciences, Indian Institute of Science Education and Research (IISER) Bhopal, Bhopal Bypass Road, Bhauri, Bhopal 462066, India.

[d]Department of Chemistry, Indian Institute of Science Education and Research (IISER) Bhopal, Bhopal Bypass Road, Bhauri, Bhopal 462066, India.

1. Materials. 5-Trifluoromethyl benzofuran-modified nucleoside analog **1** and corresponding phosphoramidite substrate **2** for solid-phase oligonucleotide (ON) synthesis were synthesized as per our previously reported procedure.[S1] *N*-acetyl-protected dC, *N*-Benzoyl-protected dA, *N,N*-dimethylformamide-protected dG, and dT phosphoramidite substrates needed for solid-phase DNA synthesis were procured from ChemGenes. Solid supports required for DNA synthesis were purchased from Glen Research. All other reagents required for solid phase ON synthesis were obtained from Sigma-Aldrich. Control DNA ONs Telo1, TeloC, **6** and **7** were purchased from Integrated DNA Technology, and purified using 18% denaturing polyacrylamide gel electrophoresis (PAGE). All other reagents (BioUltra grade) for the preparation of buffer solutions were purchased from Sigma-Aldrich. Autoclaved water was used for preparing all buffer solutions, and in all biophysical studies.

2. Instruments. NMR spectra of small molecules were acquired on a Bruker AVANCE III HD ASCEND 400 MHz spectrometer and processed using Mnova software from Mestrelab Research. Mass analysis was carried out using ESI-MS Waters Synapt G2-Si Mass Spectrometry instrument. Modified DNA oligos were synthesized on Applied Biosystems DNA/RNA synthesizer (ABI-394). RP-HPLC analysis was performed using Agilent Technologies 1260 Infinity HPLC. Absorption spectra were recorded on a UV-2600 Shimadzu spectrophotometer. Fluorescence of the ONs samples were recorded using a Fluoromax-4 spectrophotometer (Horiba Scientific). The time-resolved fluorescence of the ONs was performed using a HORIBA Delta Flex Time-Correlated Single Photon Counting (TCSPC) system using a 340 nm laser source. The fluorescence decay profile was deconvoluted by using EZ software, and decay was fitted with χ^2 values close to unity. UV-thermal melting analysis of the ONs was carried out on Cary 300 Bio UV-Vis spectrophotometer. CD measurements was done on a JASCO J-815 CD spectrometer. NMR spectra of the ONs were acquired on a Bruker AVANCE III HD ASCEND 600 MHz spectrometer equipped with Cryo-Probe (CP2.1 QCl 600S3 H/F-C/N-D-05 Z XT) and processed using Bruker TopSpin Software.

3. Solid-phase DNA ON synthesis. TFBF-dU modified DNA ONs Telo2 and **3**–**5** were synthesized in 1 µmole scale (1000 Å CPG solid support) on ABI-394 DNA/RNA synthesizer by standard solid phase synthesis protocol using phosphoramidite **2**. ON sequences with final trityl deprotection step were synthesized, and the solid supports were treated with 30% aqueous ammonium hydroxide solution for 24 h at 55 °C. Each sample was cooled on an ice bath and centrifuged. Then supernatant was transferred to a 1.5 mL Eppendorf tube, evaporated to dryness and the ON was purified by denaturing polyacrylamide gel electrophoresis (PAGE) (18% gel). Gel was irradiated with UV-light to identify the desired band corresponding to the modified ON, which was isolated and transferred to a poly-prep column (Bio-Rad). The gel pieces were crushed and soaked in aqueous ammonium acetate (0.5 M, 3 mL) for 12 h to extract the ON. Oligo was desalted using Sep-Pak C-18 cartridges (waters). The purity and integrity of modified ONs were confirmed by RP-HPLC and ESI-MS analysis.

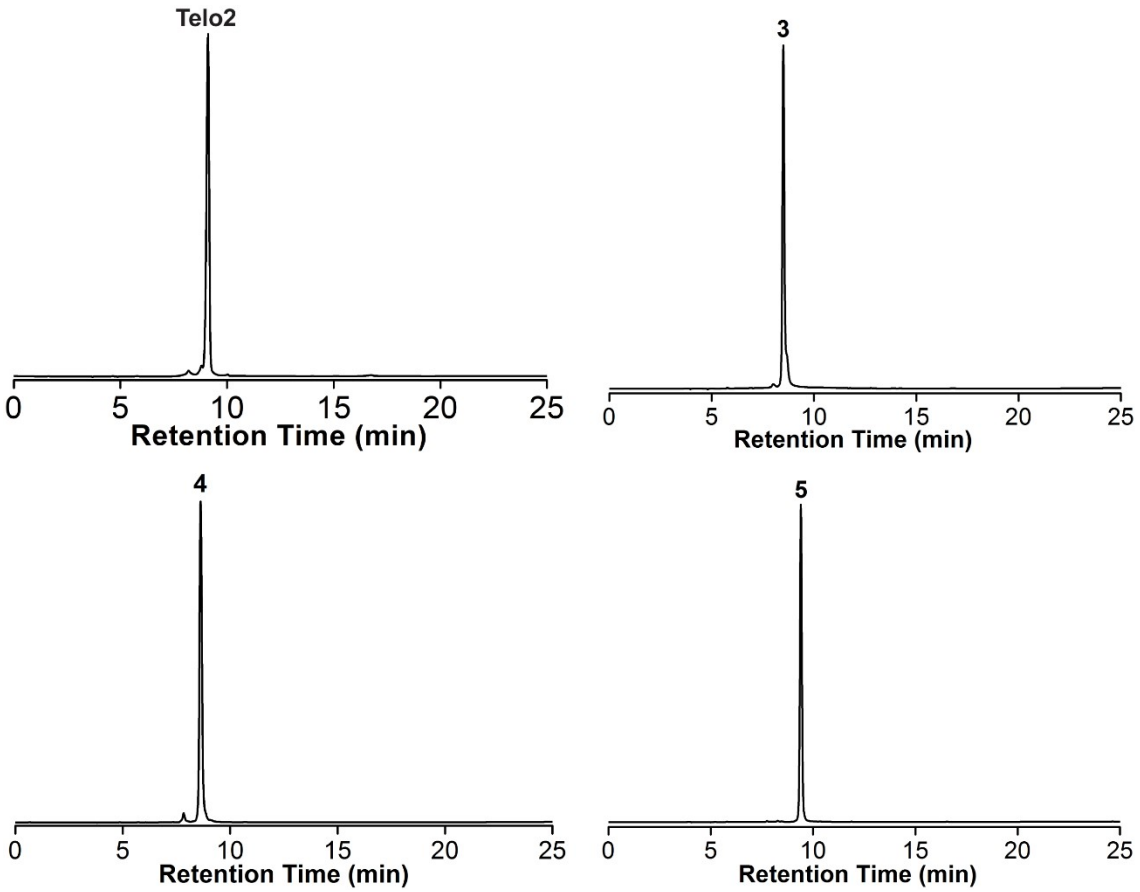

Fig. S1. RP-HPLC chromatograms of TFBF-modified Telo2 and EGFR ONs **3**–**5** analyzed at 260 nm. Mobile phase A = 50 mM triethylammonium acetate buffer (pH 7.5), mobile phase B = acetonitrile. Flow rate = 1 mL/min. Gradient = 0-100 % B in 30 min. HPLC analysis was performed using a Luna C18 column (250 x 4.6 mm, 5 micron).

4. Mass analysis of modified ON.

MALDI TOF analysis. The mass of TFBF-dU modified Telo2 was obtained using Applied Biosystems 4800 Plus MALDI TOF/TOF analyzer. A solution containing 1.5 µL of Telo2 (250 µM), 2 µL of an internal DNA standard (100 µM), 4 µL of an 8:2 solution of 3-hydroxypicolinic acid and ammonium citrate buffer (100 mM, pH 9) was desalted by adding an ionexchange resin (Dowex 50W-X8, 100-200 mesh). 2 µL of the above solution was spotted on a MALDI plate and air dried. The MALDI spectrum was referenced relative to the mass of an internal DNA standard. Internal DNA standard sequence 5' TAATACGACTCACTATAG 3', m/z of +1 and +2 ions are 5466.6 and 2733.3.

ESI-MS analysis. Mass of the modified ONs were determined by ESI-MS analysis in negative mode by injecting DNA ONs (~300 pmol) dissolved in 50% acetonitrile in an aqueous solution of 10 mM triethylamine and 100 mM hexafluoro-2-propanol.

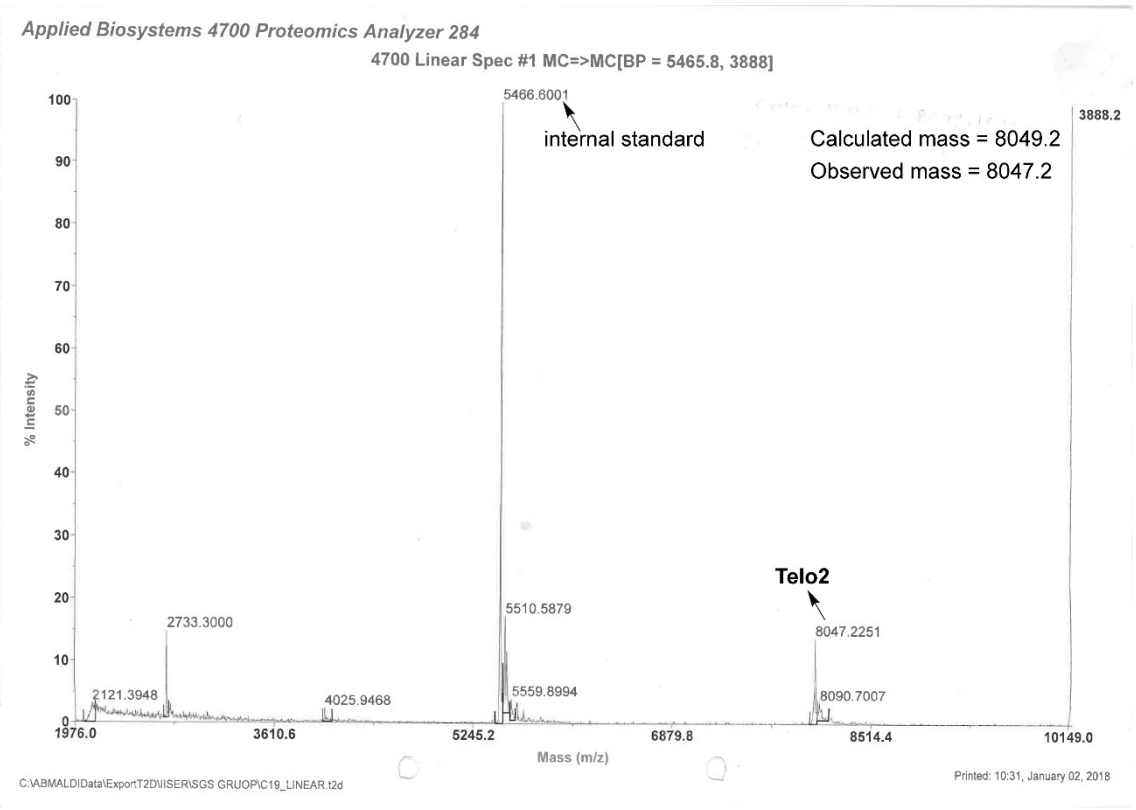

Fig. S2. MALDI-TOF MS spectrum of TFBF-modified Telo2. Internal DNA ON standard m/z of +1 and +2 ions are 5466.6 and 2733.3. See Section 4 for details.

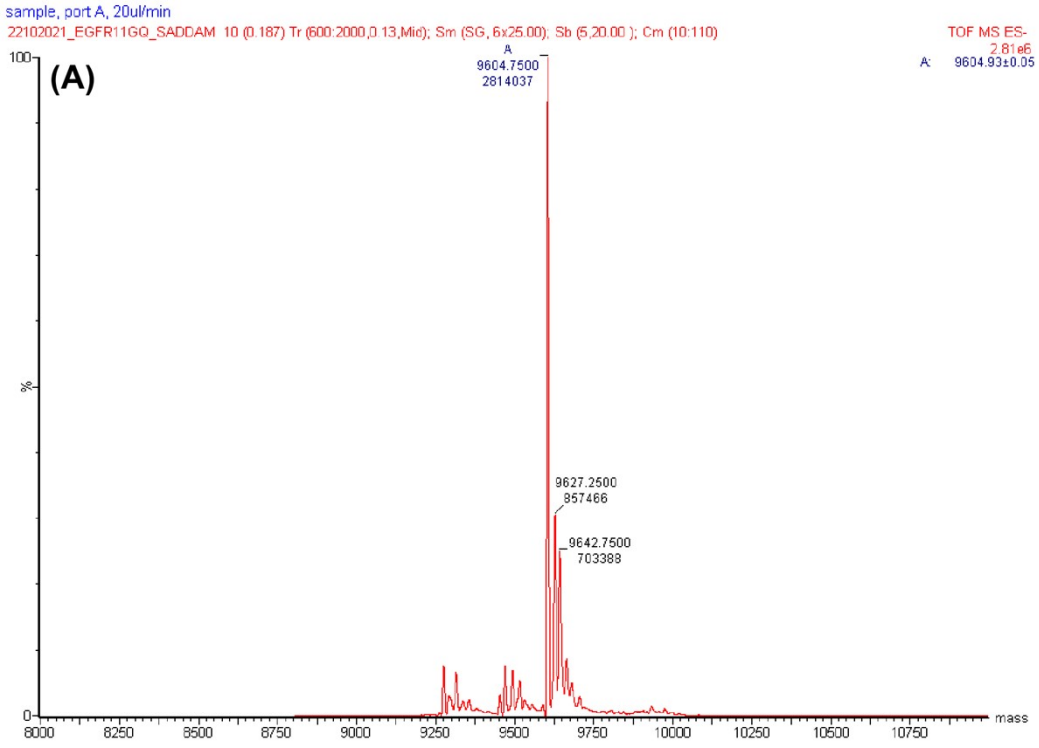
sample, port A, 20ul/min
22102021_EGFR11GQ_SADDAM 10 (0.187) Tr (600:2000,0.13,Mid); Sm (SG, 6x25.00); Sb (5,20.00); Cm (10:110)
TOF MS ES-
2.81e6
A: 9604.93±0.05
(A)
A
9604.7500
2814037
9627.2500
857466
9642.7500
703388
%
mass
100
0
8000
8250
8500
8750
9000
9250
9500
9750
10000
10250
10500
10750

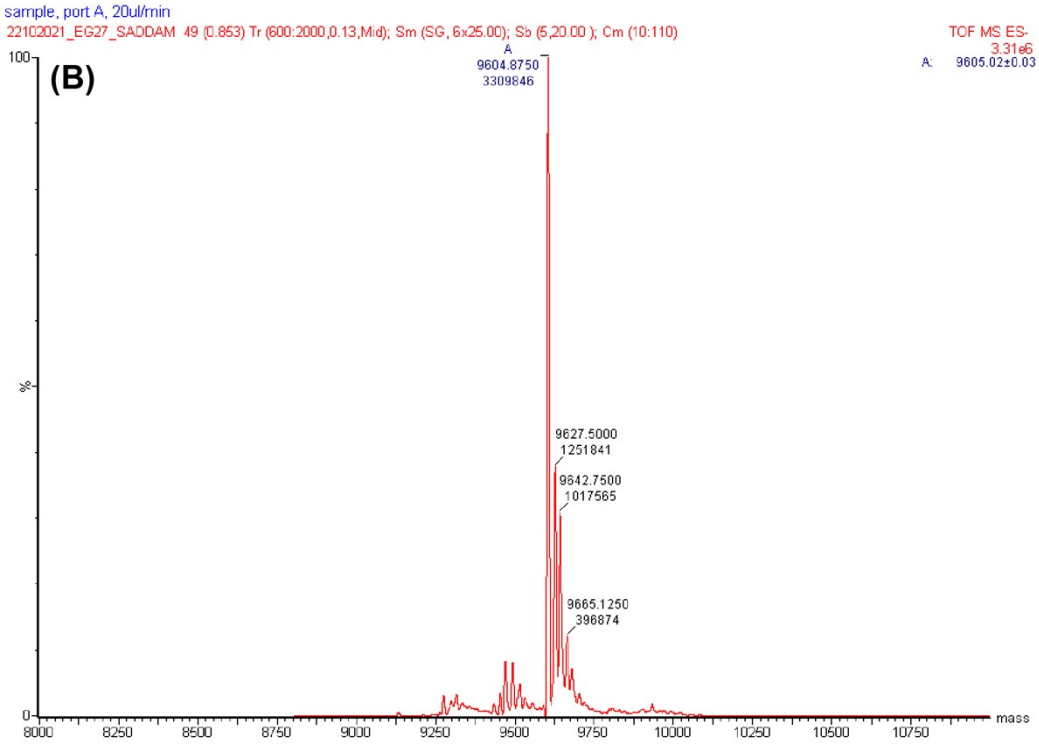
sample, port A, 20ul/min
22102021_EG27_SADDAM 49 (0.853) Tr (600:2000,0.13,Mid); Sm (SG, 6x25.00); Sb (5,20.00); Cm (10:110)
TOF MS ES-
3.31e6
A: 9605.02±0.03
(B)
A
9604.8750
3309846
9627.5000
1251841
9642.7500
1017565
9665.1250
396874
%
mass
100
0
8000
8250
8500
8750
9000
9250
9500
9750
10000
10250
10500
10750

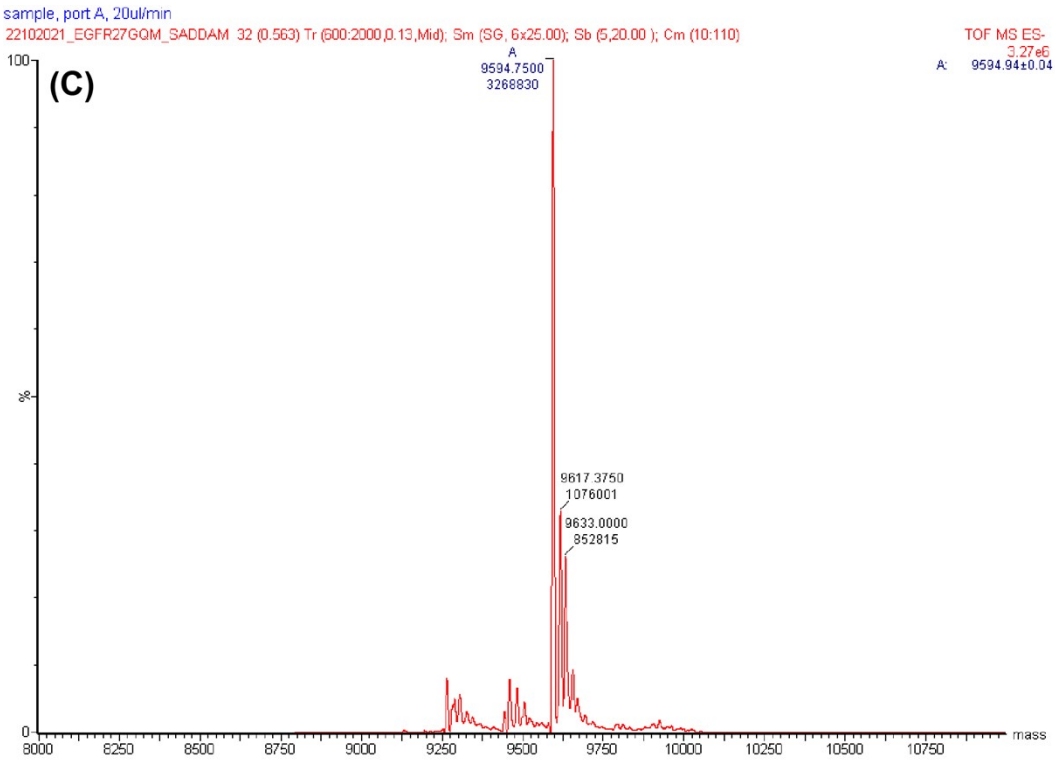

Fig. S3. ESI-MS spectra of TFBF-modified EGFR ONs (**A**) **3**, (**B**) **4**, (**C**) **5**.

Table S1. Molar absorptivity and mass of modified DNA ONs.

DNA ON	ε_{260} [a] [M^{-1} cm^{-1}]	Calculated mass	Observed mass
Telo2	256 x 10^3	8049.2	8047.2
3	295 x 10^3	9605.1	9604.8
4	295 x 10^3	9605.1	9604.9
5	297 x 10^3	9595.1	9594.8

[a]Molar absorption coefficient (ε_{260}) of the modified ONs was determined by using Oligo Analyzer 3.1. ε_{260} of modified nucleoside **1** (ε_{260} = 11.4 x 10^3 M^{-1} cm^{-1}) was used in the place of thymidine.

5. CD analysis. Samples of control Telo1 and modified Telo2 (10 µM) in 10 mM Tris.HCl buffer (pH 7.4) containing 100 mM KCl was heated at 90 °C for 3 min. To construct duplex structures, Telo1/Telo2 (10 µM) was hybridized with a complementary TeloC sequence (1:1 equiv.) in 10 mM Tris.HCl buffer (pH 7.4) containing 100 mM LiCl at 90 °C for 3 min. Similarly, EGFR DNA ONs (10 µM) samples were prepared in 10 mM Tris.HCl buffer (pH 7.4) containing different KCl concentrations or 100 mM LiCl and annealed by heating at 90 °C for 3 min. ONs samples were cooled slowly to RT and incubated overnight at RT. Samples were then diluted to a final concentration of 5 µM in 10 mM Tris.HCl buffer (pH 7.4) containing different KCl concentrations or 100 mM LiCl. CD measurements of ON samples were recorded from 310 nm to 220 nm on a JASCO J-815 CD spectrometer at 25 °C using 1 nm bandwidth. All experiments were done in

duplicate with an average of three scans for each sample. The spectrum of buffer in absence of ON was subtracted from all ON sample spectra.

6. UV-thermal melting analysis. Samples of DNA ONs were annealed in 10 mM Tris.HCl buffer (pH 7.4) containing 100 mM KCl as mentioned above. The UV-thermal melting experiment using ONs (1 µM) was performed on a Cary 300Bio UV/Vis spectrophotometer. The temperature was increased from 20 °C to 90 °C at 1 °C min^{-1} interval and changes in absorbance at 295 nm were measured at every 1 °C interval. T_m values were determined from the forward and revere cycles.

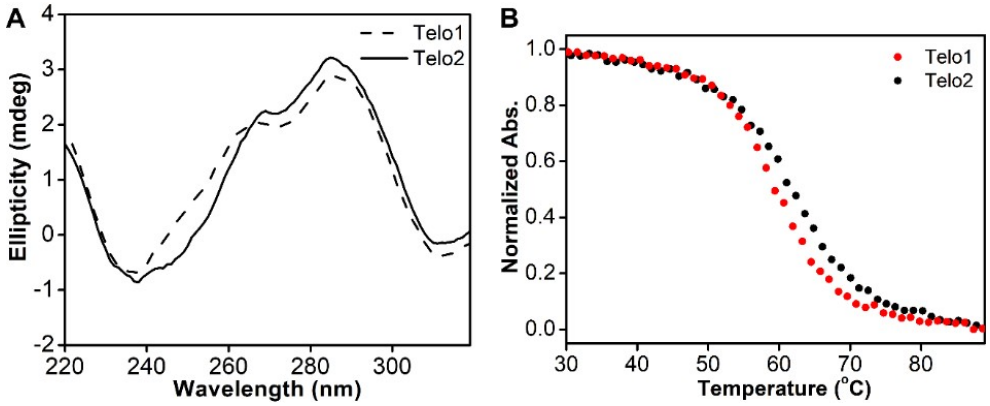

Fig. S4. (**A**) CD spectra of control Telo1 and modified Telo2 ONs (5 µM). (**B**) UV-thermal melting profile (at 295 nm) of Telo1 and Telo2 ONs (1 µM). See Section 5 and 6 for details.

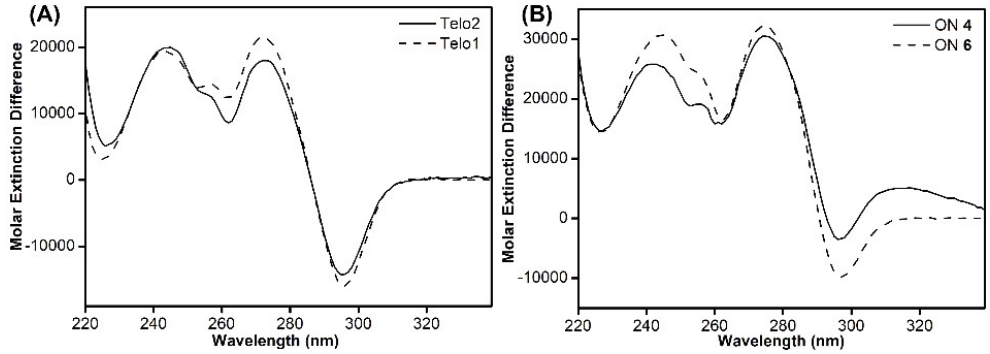

Fig. S5. Thermal difference spectrum (TDS) for Telo2 (**A**) and EGFR ON **4** (**B**), and corresponding unmodified control ON sequences. ONs samples (5 µM) were annealed in 10 mM Tris.HCl buffer (pH 7.4) containing 100 mM KCl and UV spectrum of ONs was recorded at 25 °C and 90 °C. The TDS was obtained by subtracting the UV absorption profile of the folded form from the unfolded form.

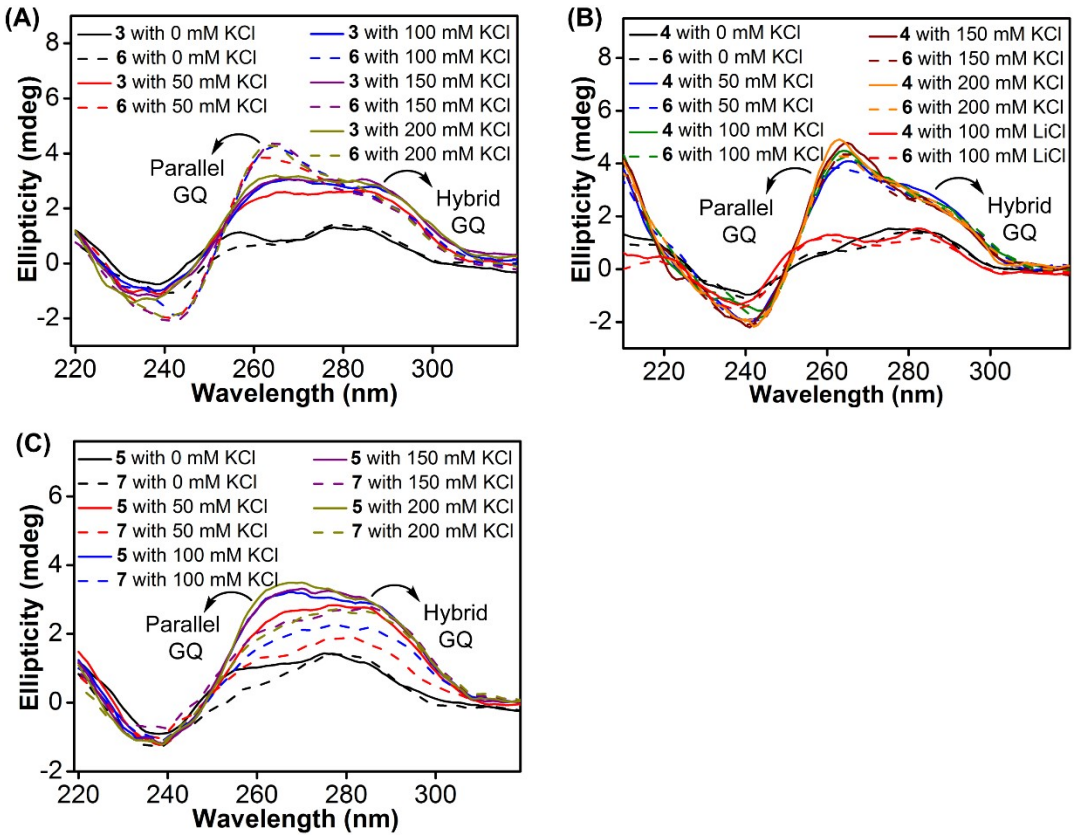

Fig. S6. (**A**, **B** and **C**) CD spectra (5 µM) of modified EGFR ONs **3**–**5** (solid lines) and their control ONs **6** and **7** (dashed lines) in different ionic conditions.

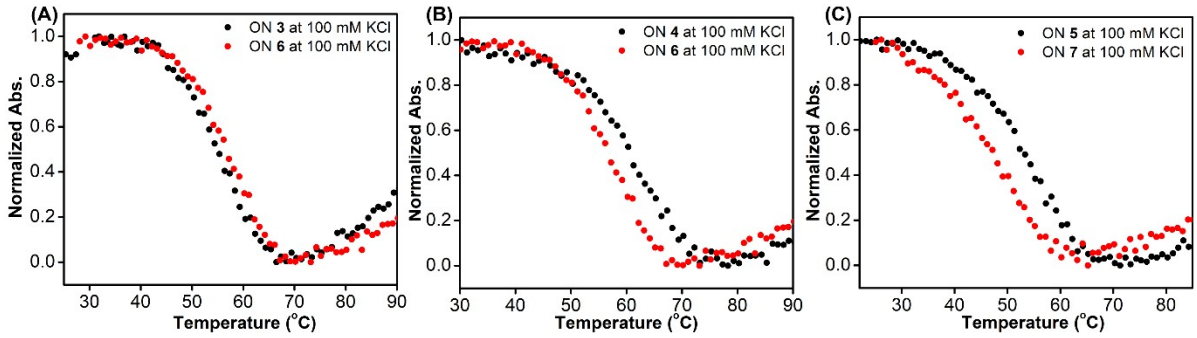

Fig. S7. UV-thermal melting profile (at 295 nm) of modified EGFR ONs **3**–**5** and corresponding control unmodified ONs **6** and **7** (1 µM).

Table S2. T_m values of modified Telo2 and EGFR ONs **3**–**5** and control unmodified Telo1 and EGFR ONs **6** and **7.**

	T_m (°C)						
KCl	Telo1	Telo2	ON **3**	ON **4**	ON **5**	ON **6**	ON **7**
100 mM	60.8 ± 0.6	60.2 ± 0.6	53.0 ± 0.6	56.3 ± 1.0	51.7 ± 1.2	54.8 ± 1.2	48.1 ± 1.0

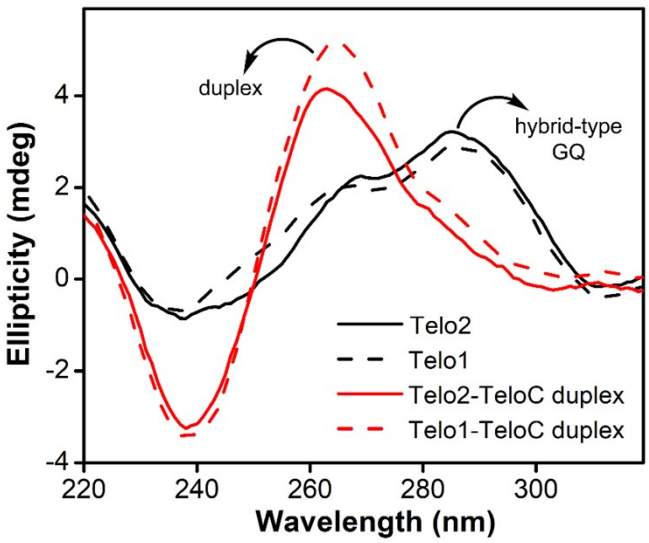

Fig. S8. A comparison of CD spectra of duplex and GQ structures formed by the telomeric repeat ONs (5 µM). See section 5 for experimental details.

7. Fluorescence and NMR studies of modified Telo2 ON.

Fluorescence. Single-stranded modified Telo2 ON was annealed in 10 mM Tris.HCl containing 100 mM KCl and its duplex was constructed by hybridizing with a complimentary TeloC sequence (1:1) in 10 mM Tris.HCl containing 100 mM LiCl. Samples were heated at 90 °C for 3 min and slowly cooled to RT. Fluorescence of DNA ON samples (1 µM) was recorded by exciting the samples at 330 nm with excitation and emission slit widths of 6 nm and 6 nm, respectively. Experiments were done in triplicate in a micro fluorescence cuvette (Hellma, path length 1.0 cm) on a Fluoromax-4 spectrofluorometer (Horiba Scientific).

NMR. The sample of Telo2 (25 µM) in 10 mM Tris.HCl buffer (pH 7.4) containing 100 mM KCl and 20% D_2O and 1:1 mixture of Telo2 and its complementary ON TeloC in 10 mM Tris.HCl buffer (pH 7.4) containing 100 mM LiCl and 20% D_2O was annealed at 90 °C for 3 min. Samples were slowly cooled to RT and transferred to a Shigemi tube (5 mm advance NMR micro-tube) for NMR analysis. ^{19}F and ^{1}H NMR spectra were acquired at a frequency of 564.9 MHz and 600 MHz, respectively, on a Bruker AVANCE III HD ASCEND 600 MHz spectrometer equipped with Cryo-Probe (CP2.1 QCl 600S3 H/F-C/N-D-05 Z XT). All ^{19}F NMR spectrum were calibrated relative to an external standard, trifluorotoluene (TFT = −63.72 ppm). Spectral parameters for ^{19}F NMR: excitation pulse: 12 µs; spectral width: 29.90 ppm; transmitter frequency offset: -60.00 ppm; acquisition time: 0.1 s; relaxation delay: 1.0 s; number of scans: 500. Using these parameters, spectra were obtained in 10 min. Each spectrum was processed with an exponential window function using lb = 15 Hz. ^{1}H NMR spectra were obtained with water suppression using excitation sculpting with gradients. Number of scans were in the range of 700.

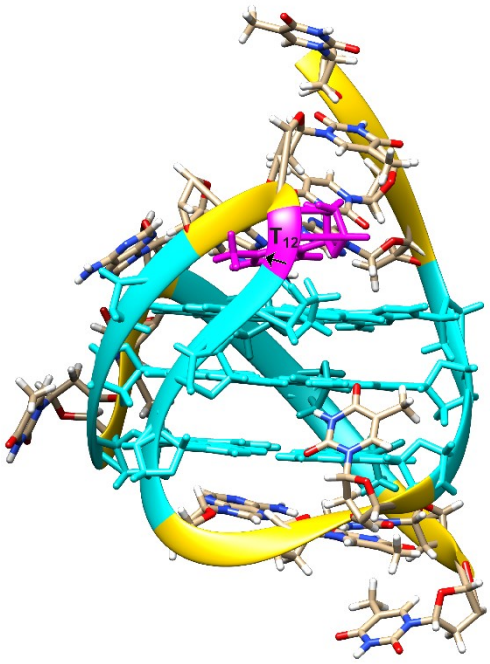

Fig. S9. NMR structure of a hybrid GQ topology of the human telomeric repeat (PDB: 2JPZ).[S2] Guanosines participating in the tetrad formation are shown in cyan. T_{12} residue is shown in magenta. Arrow shows the C5-postion of T_{12} where the TFBF heterocycle modification is placed in the modified Telo2 ON. TFBF modification does not affect the GQ structure. Hence, TFBF modification at C5-position is likely to be projected into the groove away from the G-tetrad. As a result of reduced stacking interaction, the GQ form shows higher fluorescence intensity. The figure was generated using UCSF Chimera version 1.15.

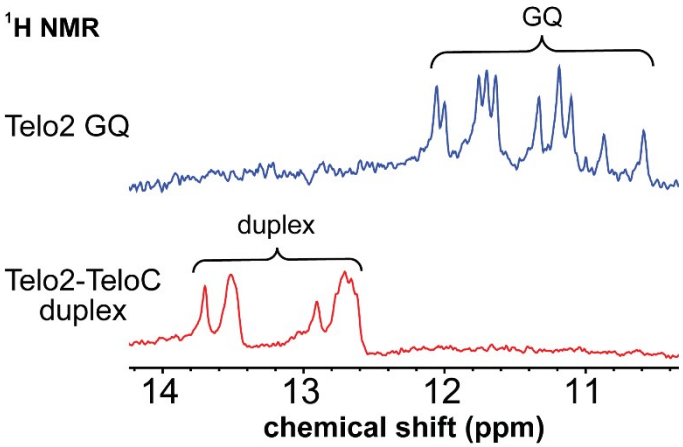

Fig. S10. ^{1}H NMR spectra of the modified telomeric ON forming GQ and duplex structures. See section 7 for details.

8. Fluorescence study of modified EGFR ONs.

Steady-state fluorescence: Samples of TFBF-dU modified ON **4** and **5** (1 µM) were prepared in 10 mM Tris.HCl (pH 7.4) buffer containing different KCl concentrations or 100 mM LiCl by using the above procedure. Additionally, control solutions of free nucleoside (TFBF-dU) (2 µM) in 10 mM Tris.HCl (pH 7.4) buffer containing different KCl concentrations or 100 mM LiCl were prepared. Fluorescence measurements were performed by exciting ONs samples at 330 nm and TFBF-dU samples at 320 nm, respectively. Excitation and emission slit widths for respective samples are provided in the figures caption. Experiments were performed in triplicate in a micro fluorescence cuvette (Hellma, path length 1.0 cm) on a Fluoromax-4 spectrofluorometer (Horiba Scientific).

Time-resolved fluorescence analysis of modified ONs. Samples of TFBF-dU modified ONs **4** and **5** (4 µM) in 10 mM Tris.HCl (pH 7.4) buffer were prepared and used for excited-state decay kinetics measurements. ONs samples were excited using a 340 nm LED source and the fluorescence decay was collected at respective emission maximum with an increase in KCl concentrations. The concentration of the KCl was increased by adding different aliquots of 3 M KCl into the ON sample and incubated for one hour before measurements. Fluorescence decay of the ON samples were deconvoluted using EZ software and fitted by an exponential decay with χ^2 value close to unity.

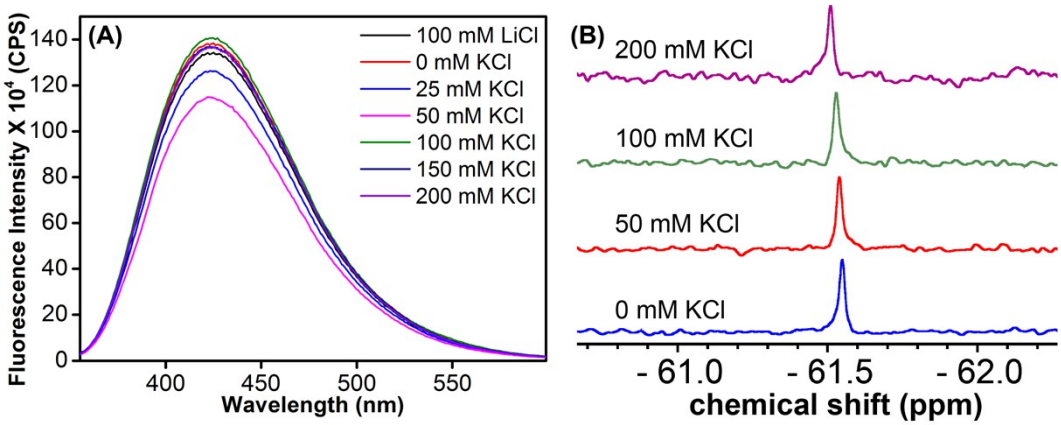

Fig. S11. (**A**) Fluorescence spectra of TFBF-dU (2 µM), and (**B**) ^{19}F-NMR spectra of TFBF-dU (10 µM) at different KCl concentrations. In the fluorescence study, samples were excited at 320 nm with excitation and emission slit widths of 5 nm and 6 nm, respectively.

9. Computational analysis. In order to generate the model for the two architectures of the EGFR G-rich sequences, a combination of 3D-NuS[S3] webserver and manual editing has been employed. For generating the hybrid architecture, the loop sequences were initially added to the 3D-NuS web server, where the hybrid GQ structure of class Q17 was generated. The 5' terminal dG was excluded in both architectures. The web server-generated structure was extracted in PDB format. The hairpin domain of the structure lacked any base pairing interaction. Therefore, the sequence of the hairpin domain was separately modeled with the help of the DNA folding form of the Mfold web server,[S4] RNAalifold web server, and 3DNA[S5]. The hairpin domain from the 3D-NuS PDB structure was removed, and the newly generated hairpin was placed with the help of PyMOL software. Further, the coordinates of the GQ and the newly generated hairpin domain were combined manually to generate a new PDB file. Similarly, for the parallel GQ, the primary

architecture was generated from the 3D-NuS web server, after which the hairpin domain was placed separately. The hairpin domain, as well as dT26 (dT27 of ON **4**), were manually placed with the help of PyMOL, and residue numbers were corrected and then saved in the PDB format.

Both the PDB structures generated were added into the Tleap module of AmberTools 21, and K^+ counter ions were added to generate the coordinate and topology files. The central K^+ ions were also added in both cases. The OL15[S6] force field was used for DNA and TIP3P water model for water and counter ions. The structures were subjected to a 100000-step minimization using the implicit solvent model in AMBER 18.[S7] The final structures after the minimization was again loaded to the tleap module. These structures were enclosed in a rectangular water box of 10 Å, and the coordinate and topology files were generated. The systems were then subjected to 10000 steps of minimization by the steepest descent method with a restraint of 2.0 kcal/mol $Å^2$ on the DNA and central K^+ ions. The minimization followed 100 ps of heating and 100 ps of density equilibration with restraints of 50 kcal/mol $Å^2$ and 2.0 kcal/mol $Å^2$. The systems were then equilibrated for 800 ps in NPT ensemble, and unrestrained MD simulation was performed using NPT ensemble for 400 ns in GPU accelerated version of PMEMD[S8-S10] in AMBER 18. SHAKE algorithm was applied to subject the hydrogen atoms to bond length constraints. Langevin[S11] thermostat with a collision frequency of 2 ps^{-1} was used to maintain the temperature at 300 K, and Berendsen[S12] barostat with a relaxation time of 2 ps was used to maintain pressure. The trajectories were visualized using UCSF Chimera[S13], and images were rendered using PyMOL. The analysis was carried out using the CPPTRAJ[S14] module of AmberTools.

The 400 ns trajectories were clustered into 5 ensembles using the hierarchical agglomerative clustering algorithm. The hybrid GQ has one major cluster which existed for ~60 % of the simulation time (Fig. S12A†), and the parallel GQ has one major cluster which existed for ~50 % (Fig. S12B†) of the simulation time. Since the 5′ terminal dG was excluded in both architectures, the numbering of the nucleotides in the ON sequence has been renumbered (Fig. 5). In the hybrid GQ, the hairpin domain maintains the two base pairs (dG19:dC25 and dC20:dG24) intact during the entire simulation, while the same is lost towards the end of the simulation in the parallel GQ. dT26 (dT27 in ON **4** and **6**) stacks with both dC25 and dG3 maintaining an average distance of 3.80 ± 0.24 Å and 4.10 ± 0.32 Å respectively in the hybrid GQ. In the case of parallel GQ, dT26 partially stacks over dG16, maintaining an average distance of 4.49 ± 1.17 Å. The center of mass of the heavy atoms of the bases (excluding sugar) was considered for the distance calculation.

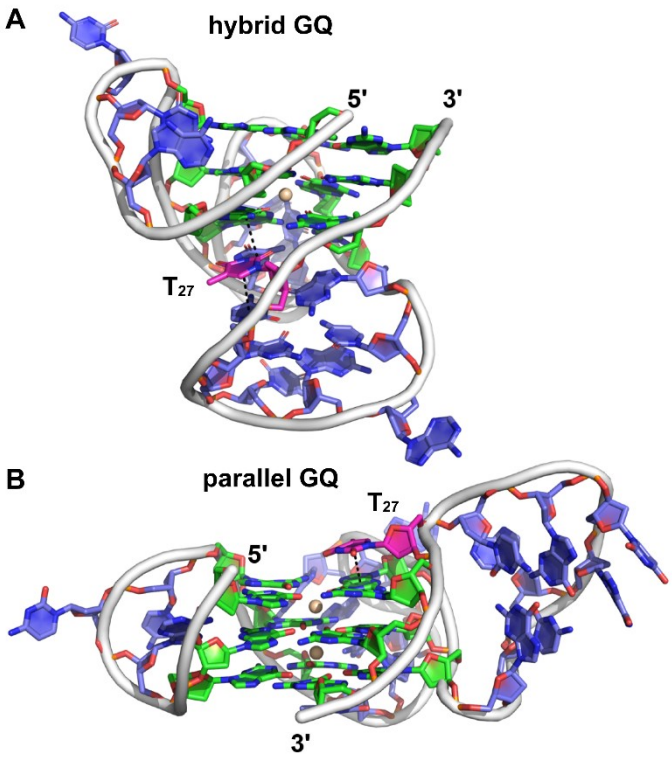

Fig. S12. Representative structure of the major cluster of (**A**) hybrid and (**B**) parallel GQ topologies. Carbon atoms of G-tetrads are represented in green, T_{27} is shown in magenta, and all other nucleotides are represented in purple. Nitrogen atoms are represented in blue, oxygen in red, and phosphate in orange. Hydrogen atoms are omitted for clarity. (**A**) In the hybrid form, T_{27} is stacked between the hairpin domain and a G-tetrad. (**B**) In the parallel form, T_{27} is partially stacked over the top G-tetrad. See Section 9 for details.

10. ^{19}F and ^{1}H NMR analysis of modified EGFR DNA ONs at different KCl. Samples of the modified DNA ONs **4** and **5** (25 µM) were prepared in 10 mM of Tris.HCl buffer (pH 7.4) containing no KCl or 100 mM LiCl and 20% D_2O and annealed by heating at 90 °C for 3 min. Samples were cooled slowly to RT and incubated overnight at RT. The sample was transferred to a Shigemi tube (5 mm advance NMR micro-tube) for NMR analysis. ^{19}F and ^{1}H NMR spectra were recorded at a frequency of 564.9 MHz and 600 MHz, respectively, on a Bruker AVANCE III HD ASCEND 600 MHz spectrometer equipped with Cryo-Probe (CP2.1 QCl 600S3 H/F-C/N-D-05 Z XT). Furthermore, aliquot of 3 M KCl was added into ON sample, and incubated for one hour after each addition and ^{19}F and ^{1}H NMR spectra were acquired with increase in KCl concentrations at 25 °C. Additionally, samples of control DNA ONs **6** and **7** (25 µM) were prepared as mentioned above and ^{1}H NMR spectra were recorded at different KCl concentrations. All ^{19}F NMR spectra were referenced relative to an external standard, trifluorotoluene (TFT = −63.72 ppm). Spectral parameters for ^{19}F NMR are same as mentioned in section 7. The ^{19}F NMR spectra were obtained in 40 min with 1500 scans. Spectra were processed with an exponential window function using lb = 10 Hz. ^{1}H NMR spectra were recorded with water suppression using excitation sculpting with gradients. Number of scans were in the range of 700.

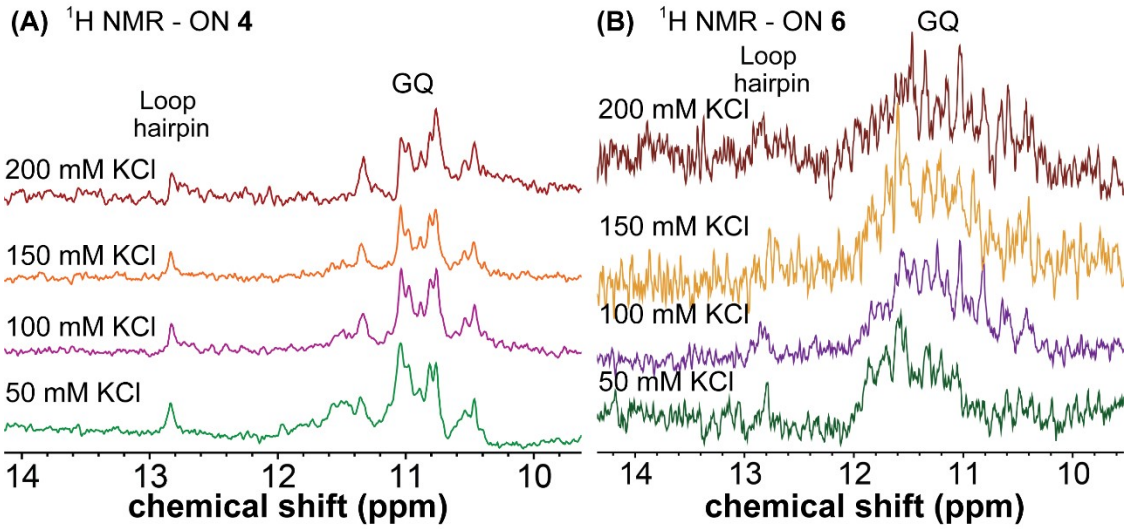

Fig. S13. ^{1}H NMR of TFBF-dU modified ON **4** and unmodified ON **6** of the native sequence.

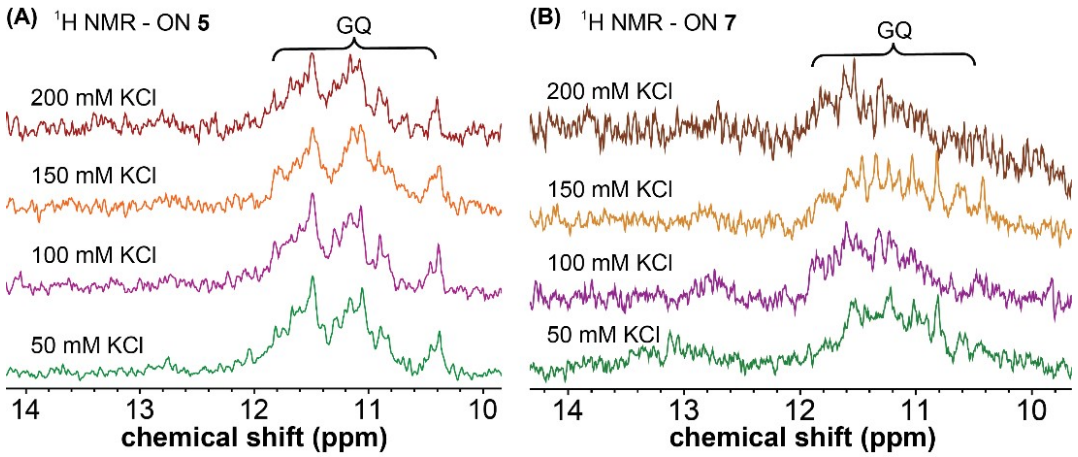

Fig. S14. ^{1}H NMR of TFBF-dU modified ON **5** and unmodified ON **7** of the mutated sequence.

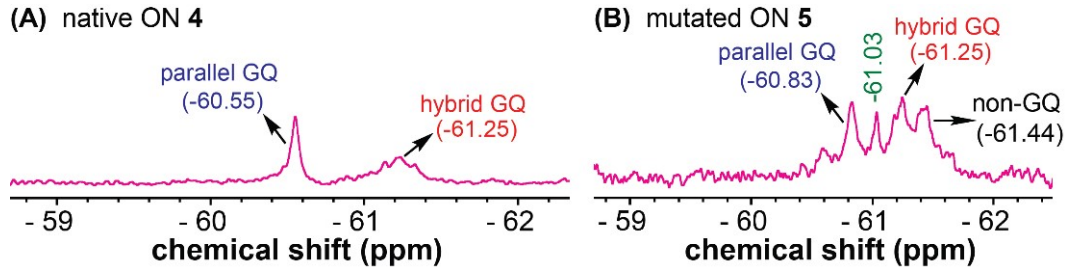

Fig. S15. ^{19}F NMR spectra of the native ON **4** and mutated ON **5** at 100 mM KCl.

11. GQ-ligand interaction by fluorescence. A series of samples of modified ON **4** (0.5 µM) in 10 mM Tris.HCl (pH 7.4) containing 100 mM KCl with increasing concentration of ligands (5 nM to 5 µM) were prepared. Samples were incubated at 4 °C for 1 h. Fluorescence emission spectra were recorded by exciting the samples at 330 nM with excitation and emission wavelength slit widths of 6 nm and 7 nm, respectively. The fluorescence of samples was recorded in triplicate reading at 25 °C. Further, the fluorescence of the blank sample containing control ON **6** and respective ligand concentration was subtracted from the individual sample reading. The apparent K_d values of ligands were determined by plotting the normalized fluorescence intensity (F_N) *vs* ligand concentration. The graph was prepared using OriginPro 8.5 software.[S15]

$$F_N = \frac{F_i - F_s}{F_0 - F_s}$$

F_i is the fluorescence intensity at each ligand titration point. F_0 and F_s are the fluorescence intensity in the absence of ligand and at saturation point, respectively. *n* is the Hill coefficient or degree of cooperativity associated with the binding.

$$F_N = F_0 + (F_s - F_0)\left(\frac{[L]^n}{[K_d]^n + [L]^n}\right)$$

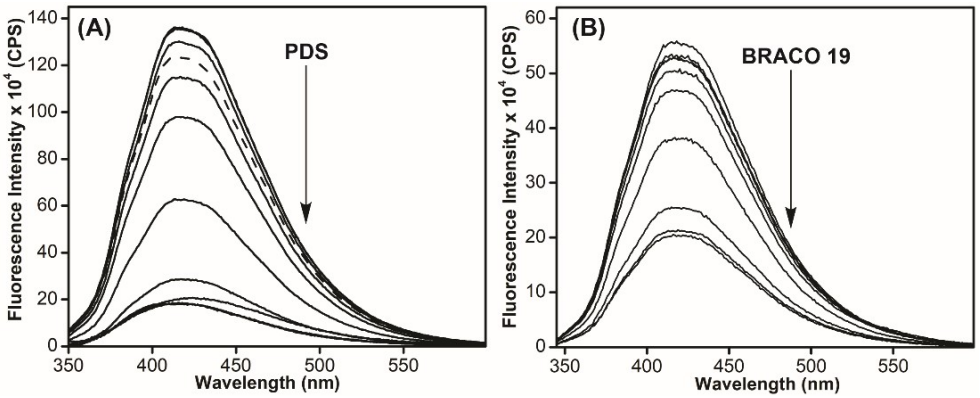

Fig. S16. Fluorescence titration of ON **4** (0.5 µM) in 10 mM Tris.HCl (pH 7.4) containing 100 mM KCl with increasing concentration of (**A**) PDS, and (**B**) BRACO-19. Fluorescence spectra of the modified ON **4** in the absence of ligands represented by a dashed line. Samples were excited at 330 nm with excitation and emission slit widths of 6 nm and 7 nm, respectively.

12. GQ-ligand interaction by UV absorption.

The samples of TMPyP4 (2 µM) were prepared in 10 mM Tris.HCl (pH 7.4) containing 100 mM KCl with increasing concentration of pre-annealed ON **4** (5 nM to 2 µM). Samples were incubated at 4 °C for 1 h and UV absorption spectra were acquired at 25 °C. Titration was performed until the wavelength and intensity of the absorption band of TMPyP4 remained unchanged.[S16,S17] UV experiment was performed in duplicate. Binding constant (K_d) was obtained from the plot of normalized absorbance (A_N) at 422 nm vs concentration of ON **4**. The graph was prepared using OriginPro 8.5 software.

$$A_N = \frac{A_i - A_s}{A_0 - A_s}$$

A_i is the absorbance intensity at each titration point. A_0 and A_s are the absorbance intensity in the absence of ON **4** and at saturation point, respectively. n is the Hill coefficient or degree of cooperativity associated with the binding.

$$A_N = A_0 + (A_s - A_0)\left(\frac{[ON]^n}{[K_d]^n + [ON]^n}\right)$$

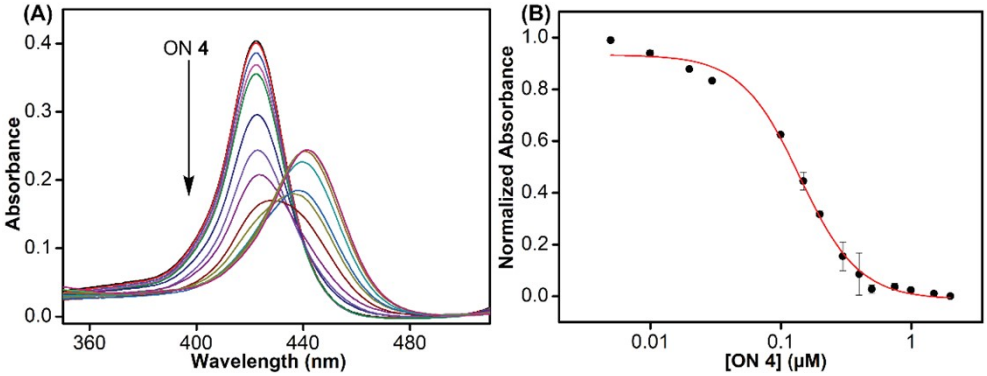

Fig. S17. (**A**) UV-vis absorption spectra. Titration of TMPyP4 (2 μM) in 10 mM Tris.HCl (pH 7.4) containing 100 mM KCl with increasing concentration of ON **4** (5 nM to 2 μM). (**B**) Curve fit plotted for normalized absorbance of TMPyP4 at 422 nm with increasing concentrations of ON **4**.

13. GQ-ligand interaction by ^{19}F NMR. Modified ON **4** (15 μM) in 10 mM Tris.HCl buffer (pH 7.4) containing 100 mM KCl and 20% D_2O was prepared and ^{19}F NMR spectra (ns = 4000) of the sample was recorded with increasing concentration of ligand (0–60 μM). Spectral parameters are the same as mentioned in Section 7 and the data was processed with an exponential window function using lb = 20 Hz.

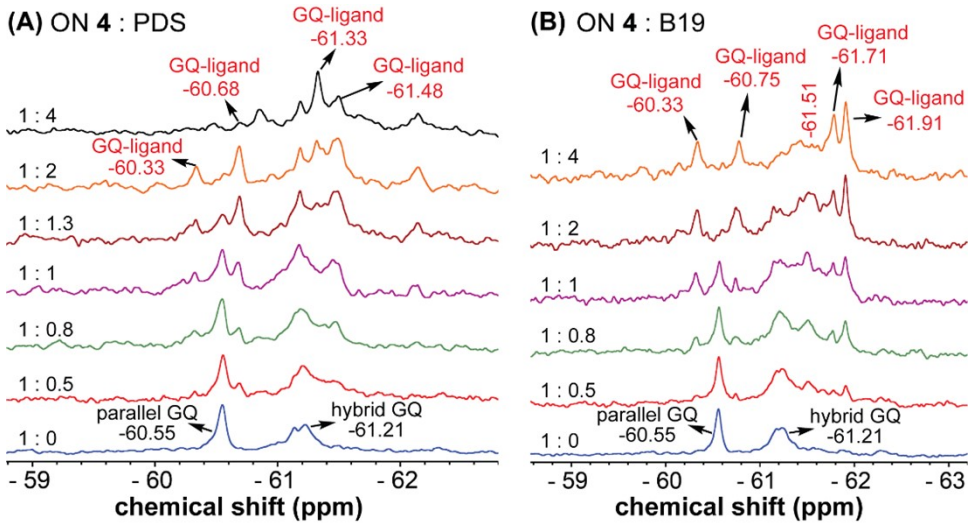

Fig. S18. ^{19}F NMR of modified ON **4** (15 µM) in Tris.HCl buffer (pH 7.4) containing 100 mM KCl with increasing concentrations of (**A**) PDS, and (**B**) BRACO-19 (B19).

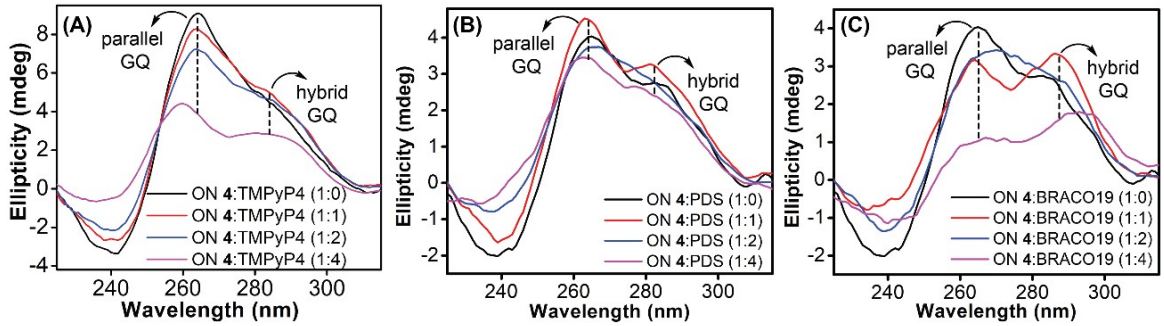

Fig. S19. (**A**) CD spectra of modified ON **4** (10 µM) upon addition of increasing concentrations of TMPyP4. CD of modified ON **4** (5 µM) at different concentrations of (**B**) PDS, and (**C**) BRACO-19.

14. Preparation of EGFR GQ (ON 4) sample for ^{19}F NMR analysis in intraoocyte buffer, lysate and egg extract.

Intraoocyte buffer. Modified ON **4** (50 µM) was annealed in an intraoocyte buffer (25 mM HEPES pH = 7.5, 110 mM KCl, 10.5 mM NaCl, 130 nM $CaCl_2$, 1 mM $MgCl_2$, 0.1 mM EDTA)[S18] containing 20% D_2O at 90 °C for 3 min. The sample was cooled slowly to RT and incubated for 1 h at RT. The ^{19}F (number of scans = 1000) and ^{1}H NMR (number of scans = 1500) spectra were recorded at a frequency of 564.9 MHz and 600 MHz at 25 °C, respectively. Spectral parameters are the same as mentioned in section 7 and the ^{19}F NMR data was processed with an exponential window function using lb = 20 Hz.

Oocytes were surgically removed from anesthetized adult female *Xenopus laevis* in accordance with a protocol approved by the Institutional Animal Ethics Committee (IAEC), IISER Bhopal.

Clear lysate.[S18] Healthy *Xenopus laevis* stage V/VI oocytes (~275) were selected and suspended in a Petri dish containing Ori-Ca^{2+} buffer (5 mM HEPES pH = 7.5, 110 mM NaCl, 5 mM KCl, 2 mM $CaCl_2$, and 1 mM $MgCl_2$). The Petri dish was kept on an ice bath for 15 min. The oocytes were washed with ice-cold intraoocyte buffer (3 x 10 mL) and resuspended in the same buffer. Oocytes were transferred in an Eppendorf tube, allowed them to settle down and the supernatant was removed carefully without disturbing the settled oocytes. Oocytes were rinsed with intraoocyte buffer (200 µL) containing 20% D_2O and then removed (this step was performed twice). Finally, 200 µL of intraoocyte buffer containing 20% D_2O was added to the Eppendorf tube containing oocytes, which were then mechanically crushed. The suspension was centrifuged at 20000g for 20 min at 4 °C, the interphase layer was carefully transferred into another Eppendorf and heated at 95 °C for 10 min. The solution was centrifuged at 20000g for 10 min at 4 °C and the clear lysate (285 µL) was transferred to another Eppendorf tube. 1 mM of preannealed ON **4** (15 µL) in an intraoocyte buffer supplemented with 20% D_2O was added to the clear lysate (final ON concentration = 50 µM). The sample was incubated at 4 °C for 30 min and transferred to a Shigemi tube (5 mm advance NMR micro-tube) for NMR analysis. ^{19}F (number of scans = 2000)

and ^{1}H NMR (number of scans = 3072) spectra were acquired at a frequency of 564.9 MHz and 600 MHz at 25 °C, respectively. Spectral parameters are the same as mentioned above. The ^{19}F NMR plot was processed with an exponential window function using lb = 20 Hz.

Egg extract. [S19] Oocytes (~900) were kept in a Petri dish containing Ori Ca^{2+} buffer (pH 7.5) for 15 min on an ice bath. The oocytes were washed with ice-cold intraoocyte buffer (3 x 20 mL) and transferred to an Eppendorf tube. The buffer just above the oocytes was removed carefully and oocytes were washed with intraoocyte buffer (400 µL) containing 20% D_2O (two times). The oocytes were centrifuged at 400g for 1 min at 4 °C and the supernatant buffer was removed. The oocytes were resuspended in the intraoocyte buffer (100 µL) containing 30% D_2O and centrifuged at 12000g for 5 min at 4 °C. The eggs were mechanically crushed and the suspension was centrifuged at 12000g for 30 min at 4 °C to obtain the interphase layer. This crude egg extract thus obtained was directly used in the NMR analysis. 1 mM of the preannealed ON **4** (15 µL) in an intraoocyte buffer containing 20% D_2O was added to the above crude egg extract (285 µL) and incubated for 30 min at 4 °C. The ^{19}F (number of scans = 3500) and ^{1}H NMR (number of scans = 4000) spectra were recorded at a frequency of 564.9 MHz and 600 MHz at 25 °C, respectively. Spectral parameters are the same as mentioned above. The ^{19}F NMR spectrum was processed with an exponential window function using lb = 20 Hz.

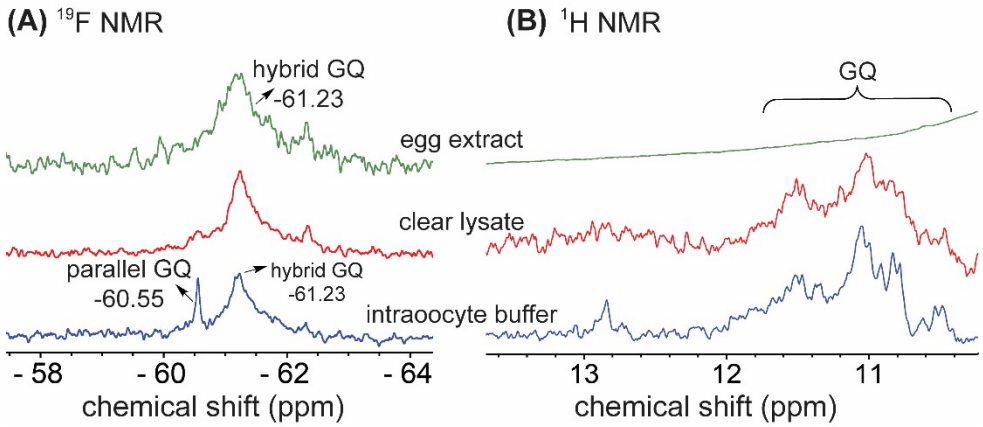

Fig. S20. ^{19}F and ^{1}H NMR spectra of ON **4** (50 µM) in intraoocyte buffer (blue), lysate (red) and egg extract (green). See section for 13 details.

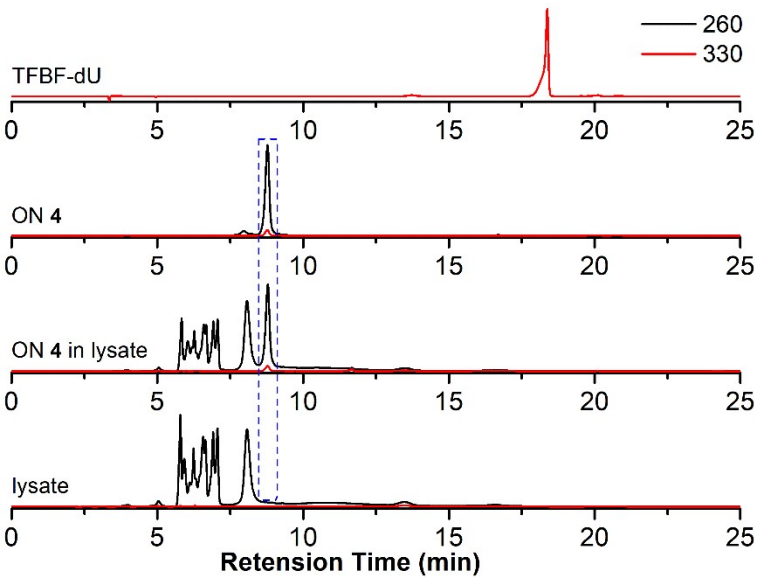

Fig. S21. Comparison of HPLC chromatograms of lysate, lysate containing ON **4** (after recording NMR), ON **4** and modified nucleoside analog (TFBF-dU). There was no detectable degradation of ON **4** in lysate.

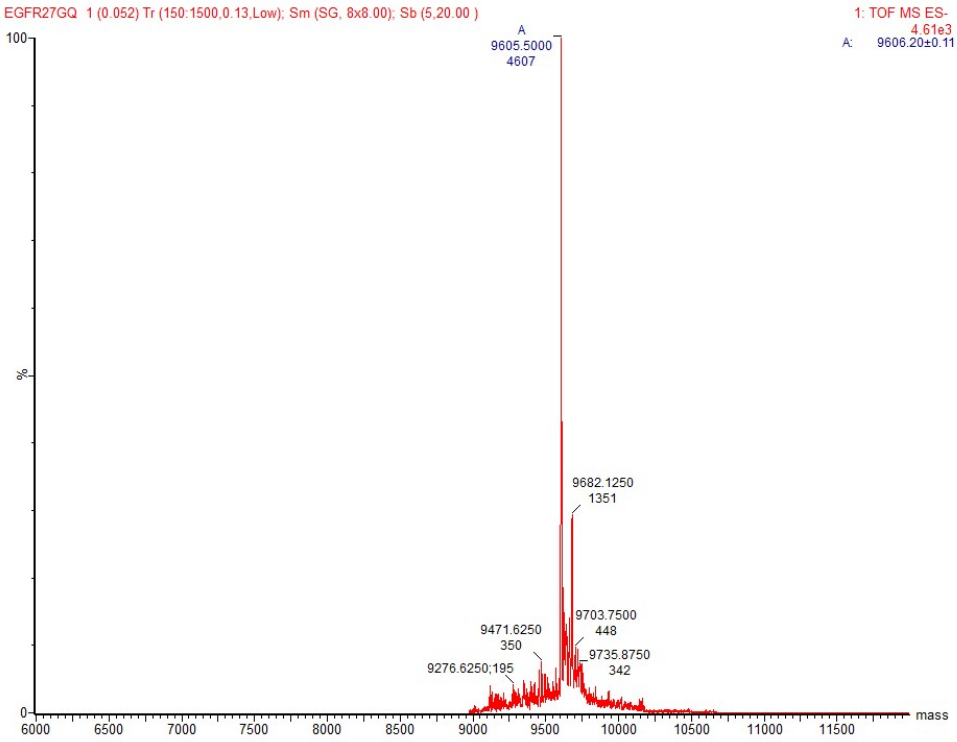

Fig. S22. ESI-MS spectra of modified ON **4** extracted from lysate sample after NMR analysis. (calculated mass = 9605.1, observed mass = 9605.5).

15. *Taq* polymerase stop assay. 5'-FAM-labeled primer (5 µM) and template DNA (**T_1–T_3**) (6 µM) were annealed in 10 mM Tris.HCl buffer containing 100 mM KCl by heating at 90 °C for 5 min. Samples were cooled slowly to RT and incubated on an ice batch for 1 h. The primer-DNA duplexes were diluted to a final concentration of 1 µM in 10 mM Tris.HCl buffer containing 100 mM KCl. Replication reaction was performed on a 20 µL reaction volume containing duplex (50 nM), dNTPs (500 µM), KCl (100 mM), 1X DNA polymerase buffer.[S20] The reaction mixture was incubated at 37 °C for 20 min and the reaction was initiated by adding 0.5 µL of Taq DNA polymerase (5 U/µL, *New England Biolabs*, Catlog. M0273S). The reaction was quenched at different time points by adding 10 µL of gel loading buffer (80% formamide by volume, 10 mM NaOH, 0.005% bromophenol blue (w/v)) and flashed cooled on a dry ice bath. The reaction mixture was concentrated on a speed-vac concentrator and analysed on a 15 % denaturing polyacrylamide gel. The gel was imaged by using a Typhoon gel scanner at FAM wavelength.

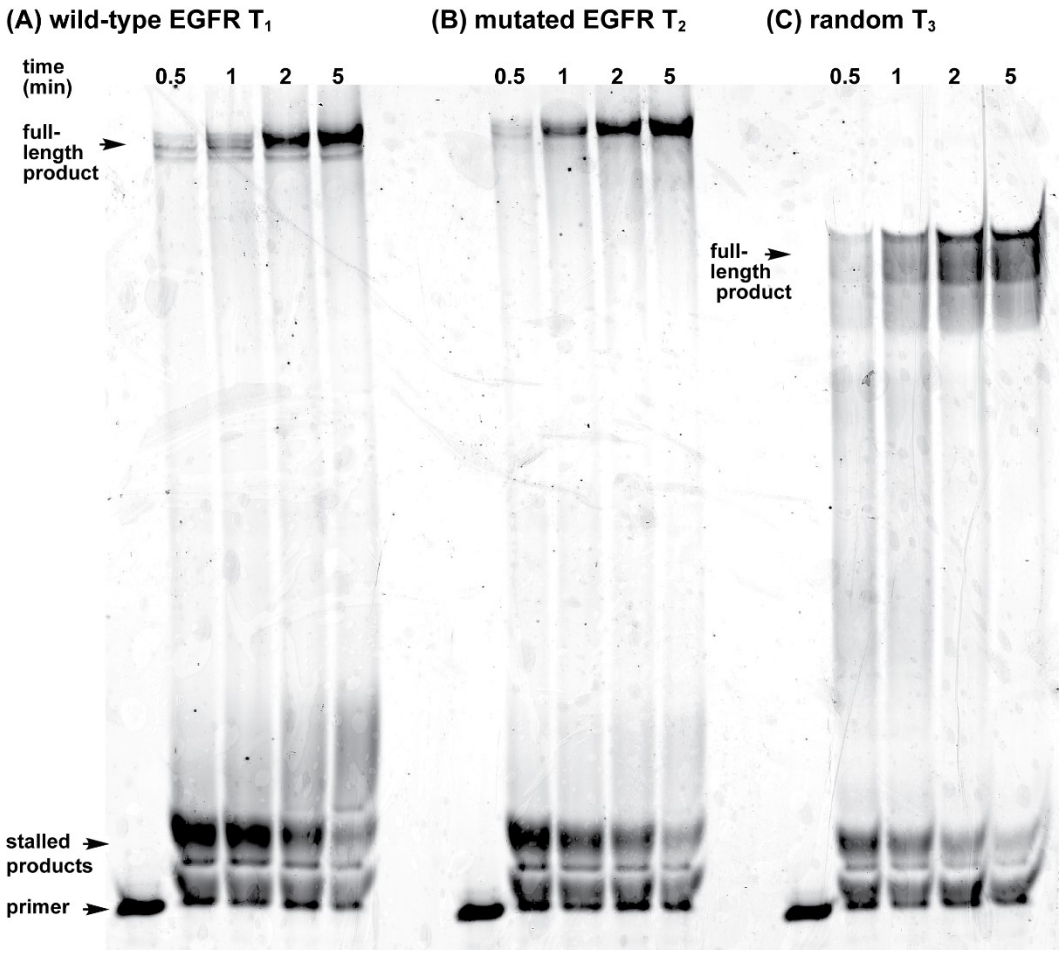

Fig. S23. PAGE analysis of the replication reactions using (**A**) a wild-type EGFR G-rich template $\mathbf{T_1}$, (**B**) a mutated EGFR G-rich template $\mathbf{T_2}$, and (**C**) a random non-GQ forming template $\mathbf{T_3}$.

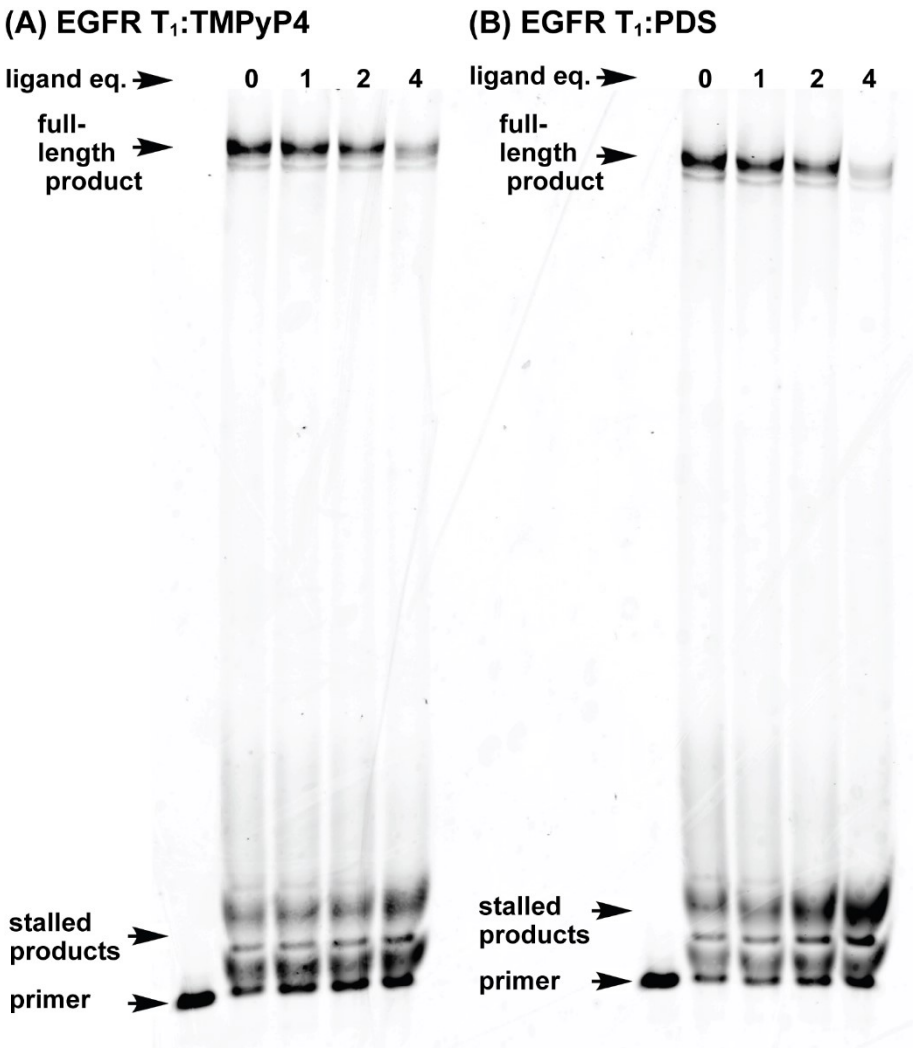

Fig. S24. PAGE analysis of the replication reactions using a wild-type EGFR $\mathbf{T_1}$ with increasing concentrations of the ligands (**A**) TMPyP4, (**B**) PDS.

16. References

S1. S. Y. Khatik and S. G. Srivatsan, *Bioconjugate Chem.*, 2022, **33**, 1515–1526.

S2. J. Dai, M. Carver, C. Punchihewa, R. A. Jones and D. Yang, *Nucleic Acids Res.*, 2007, **35**, 4927–4940.

S3. L. P. P. Patro, A. Kumar, N. Kolimi and T. Rathinavelan, *J. Mol. Biol.*, 2017, **429**, 2438–2448.

S4. M. Zuker, *Nucleic Acids Res.*, 2003, **31**, 3406–3415.

S5. X.-J. Lu and W. K. Olson, *Nat. Protoc.*, 2008, **3**, 1213–1227.

S6. R. Galindo-Murillo, J. C. Robertson, M. Zgarbová, J. Šponer, M. Otyepka, P. Jurečka and T. E. Cheatham, *J. Chem. Theory Comput.*, 2016, **12**, 4114–4127.

S7. D. A. Case, I. Y. Ben-Shalom, S. R. Brozell, D. S. Cerutti, T. E. Cheatham III, V. W. D. Cruzeiro, T. A. Darden, R. E. Duke, D. Ghoreishi and M. K. Gilson, AMBER 2018; 2018. *Univ. California, San Fr.* **2018**.

S8. R. Salomon-Ferrer, A. W. Götz, D. Poole, S. L. Grand and R. C. Walker, *J. Chem. Theory. Comput.*, 2013, **9**, 3878–3888.
S9. A. W. Götz, M. J. Williamson, D. Xu, D. Poole, S. L. Grand and R. C. Walker, *J. Chem. Theory Comput.*, 2012, **8**, 1542–1555.
S10. S. Le Grand, A. W. Götz and R. C. Walker, *Comput. Phys. Commun.*, 2013, **184**, 374–380.
S11. P. Turq and F. Lantelme, *J. Chem. Phys.*, 1977, **66**, 3039–3044.
S12. H. J. C. Berendsen, J. P. M. Postma, W. F. Van Gunsteren, A. DiNola and J. R. Haak, *J. Chem. Phys.*, 1984, **81**, 3684–3690.
S13. E. F. Pettersen, T. D. Goddard, C. C. Huang, G. S. Couch, D. M. Greenblatt, E. C. Meng and T. E. Ferrin, *J. Comput. Chem.*, 2004, **25**, 1605–1612.
S14. D. R. Roe and T. E. Cheatham III, *J. Chem. Theory Comput.*, 2013, **9**, 3084–3095.
S15. S. Manna, D. Sarkar and S. G. Srivatsan, *J. Am. Chem. Soc*., 2018, **140**, 12622–12633.
S16. N. V. Anantha, M. Azam and R. D. Sheardy, *Biochemistry*, 1998, **37**, 2709–2714.
S17. C. Wei, G. Jia, J. Yuan, Z. Feng and C. Li, *Biochemistry*, 2006, **45**, 6681-6691.
S18. R**.** Hänsel, S. Foldynová-Trantírková, F. Löhr, J. Buck, E. Bongartz, E. Bamberg, H. Schwalbe, V. Dötsch and L. Trantírek, *J. Am. Chem. Soc.*, 2009, **131**, 15761–15768.
S19. R. Hänsel, F. Löhr, S. Foldynová-Trantírková, E. Bamberg, L. Trantírek and V. Dötsch, *Nucleic Acids Res.*, 2011, **39**, 5768–5775.
S20. G. Wu and H. Han, *Methods Mol. Biol.*, 2019, **2035**, 223–231.